NUMERICAL MODELLING OF A LOW CONCENTRATION CHEMICAL SPECIES OR CONTAMINANT IN A VENTILATED, HEATED, TWO-DIMENSIONAL ROOM

BY

S.N. CHIN
ROBERT W. BESANT
DEPT. OF MECHANICAL ENGINEERING

AND

R. MANOHAR
DEPT. OF MATHEMATICS

UNIVERSITY OF SASKATCHEWAN
SASKATOON, SASKATCHEWAN
S7N 0W0

Presented at the Fifth Canadian Symposium of Fluid Dynamics

SUMMARY

In this investigation, air quality and thermal confort in two-dimensional ventilated air spaces of several geometries are numerically predicted when conditions on the various room surfaces are taken to be either adiabatic (or no mass transfer) or constant temperature (or constant concentration). Various flow conditions as specified by the Reynolds number, Prandtl number, and Archimedes number are included in the numerical results.

The method of analysis involved using the equations of fluid motion, heat transfer, and mass transfer, expressed in finite difference form and solved using an explicit method of solution and an assumed initial distribution of properties. A grid with 51 x 21 nodal points was used.

The computer model was checked for its accuracy and validated against simple analytical solutions for simple geometries and against numerical laminar flow solutions for more complex geometries. Agreement was within the numerical uncertainties. Double precision was used in the study.

The investigation was extended to turbulent flows for the case of constant eddy thermal diffusivity and mass diffusion coefficient.

The results are presented for the distribution of laminar and turbulent vorticity, stream function, temperature, and concentration profiles for a number of different flow rates, geometries, and boundary conditions. Heat transfer and mass transfer rates are computed along internal transfer surfaces.

The graphical results show regions where ventilation discomfort could exist due to high or low temperatures or excessive concentration of contaminants such as dust, water vapour, ammonia gas, etc. Such information could be important in the design and operation of indoor spaces for people or animals.

1. INTRODUCTION

The field of velocity, temperature, and particle movement or spatial variation in a ventilated air space are not, in general, independent of each other. These must be regarded as interactive processes. For example, temperature gradients that are present as a result of heat sources may induce changes in the velocity and particle concentration field. Also fluid momentum will influence the effects of buoyancy. In the case of turbulent flows, the motion induced by thermal instabilities may cause the level of turbulent mixing to increase significantly where the potential energy of natural convection is converted in part into increased turbulence levels and mass and thermal mixing. In the same manner, the mass concentration source of particles may induce instability in the air movement and, thus, increase mixing which may give rise to evenly distributed concentration fields within the airspace. Thus, the concentration, temperature, and velocity distributions may be affected by the room geometry and the location of gravitational instabilities for heat and contaminants as well as the momentum of the inlet jet and exhaust outlet. To actually model the physical events in ventilated air spaces, it is necessary to consider all the interacting factors.

The most exact theoretical approach is to treat the ventilated air as a continuum and describe the physical phenomena within the airspace by a set of partial differential equations with the appropriate boundary conditions. In general, non-linearities in the equations and variable properties make analytical solutions of these mixed-type of coupled equations impossible except for a few cases. Consequently, numerical methods present the only practical means of obtaining solutions of complex ventilation problems.

Ventilation rates adequate for satisfactory control of excess temperature, humidity, and contaminant concentrations normally occur in flow regimes that encompasses the whole range of laminar, transitional, and turbulent flow. The turbulent fluctuations range in size from some fraction of the main dimensions of the physical system down to 1 mm in length and the frequency range in the order of 1 to 10^5 cycles per second. It is evident that very large numbers of grid points are needed to accurately model the turbulent flow fluctuations in a ventilated airspace. Time average values of the turbulent properties are of interest since it is reasonable to assume that variations in the mean value over a given distance is considerably smaller than fluctuations of the instantaneous values. However, further equations or theories are needed to evaluate the turbulent transport terms. A simple approximation is Reynolds analogy (Lumley and Panosky, 1964) and assuming that the resulting eddy viscosity, conductivity, and diffusivity are constant. For turbulent flows, these eddy transport coefficients are, in general, orders of magnitude larger than the molecular diffusion coefficients. The eddy coefficients are, however, functions of locations and flow stability, and their determination is extremely difficult. The ventilation problem is further complicated by the coexistence of laminar and turbulent flows in adjacent regions within the airspace and they may change with time.

In a study of buoyancy affected flows in ventilated rooms, Nielson et.al (1979) used a turbulence model developed by Launder et.al (1973) Two extra transport equations were needed to account for the transfer of kinetic energy and energy dissipation. The relationships of the turbulent stress terms to the

eddy coefficients required the use of six empirical parameters to close the problem. These empirical constants were optimized from general fluid mechanics problems with no changes made with regard to predicting the air motion in a ventilated room. Timmons (1979) assumed that the flow condition in a ventilated airspace may fit an inviscid model. This inviscid model is based on relationships derived from jet theory for jet entrainment, jet expansion, and jet vorticity. This approach assumes that vorticity values will not change along a given streamline, whereas in viscous flow the vorticity may not remain constant along a streamline. Vorticity is introduced at the inlet and vorticity produced within the enclosure is modelled separately since the surfaces are assumed to be inviscid. Fromm (1970) in a numerical study of buoyancy driven flows in room enclosures intentionally sought to obtain solutions for high Rayleigh number flows without recourse to modelling with mean flow equations. Three-dimensional effects in turbulent flow models are perhaps even more controversal in spite of the fact that turbulent flows are inherently three dimensional. Notably, there is no general agreement on the appropriate modelling of ventilation problems.

Instead of using complicated turbulence model, Fromm's approach is used in this study; physical events in a two-dimension, ventilated airspace is assumed to be similar to a time-dependent, separated laminar flow with constant properties. Qualitative representation of mixed turbulent flow effects may be obtained by extending the problem for inlet conditions for high Reynolds number flows. Even with this restriction, the approach is thought to be representative since it considers the essential features of two-dimensional motion; namely, the effect of sharp corners on the flow, vorticity generation, diffusion and its convection. The ventilation problem is then reduced to an initial-boundary value problem of the Navier-Stokes equations and related transport equations of heat and low concentration mass transfer of a gaseous or particle contaminant.

2. THE VENTILATION MODEL

Consider a two-dimensional imcompressible, constant density newtonian fluid such as air entering a typical room geometry BCEF uniformly through an inlet supply port AF at a steady rate from impulsive start at rest as shown in Figure 2.1. The flow exit at the return port DC is considered to be far enough downstream to allow the flow to develop into a two-dimensional internal flow. The region of flow is bounded below by the floor and above by the ceiling. The interacting effects of heat and mass transfer in the developing flow field are considered for a line source operating at the floor BC. Low concentration contaminant and heat is introduced at the inlet port as specified functions of the inlet height h. At time zero, the line source and inlet flow source begin to diffuse the contaminant and heat away, thus, perturbing the assumed initial concentration and temperature fields.

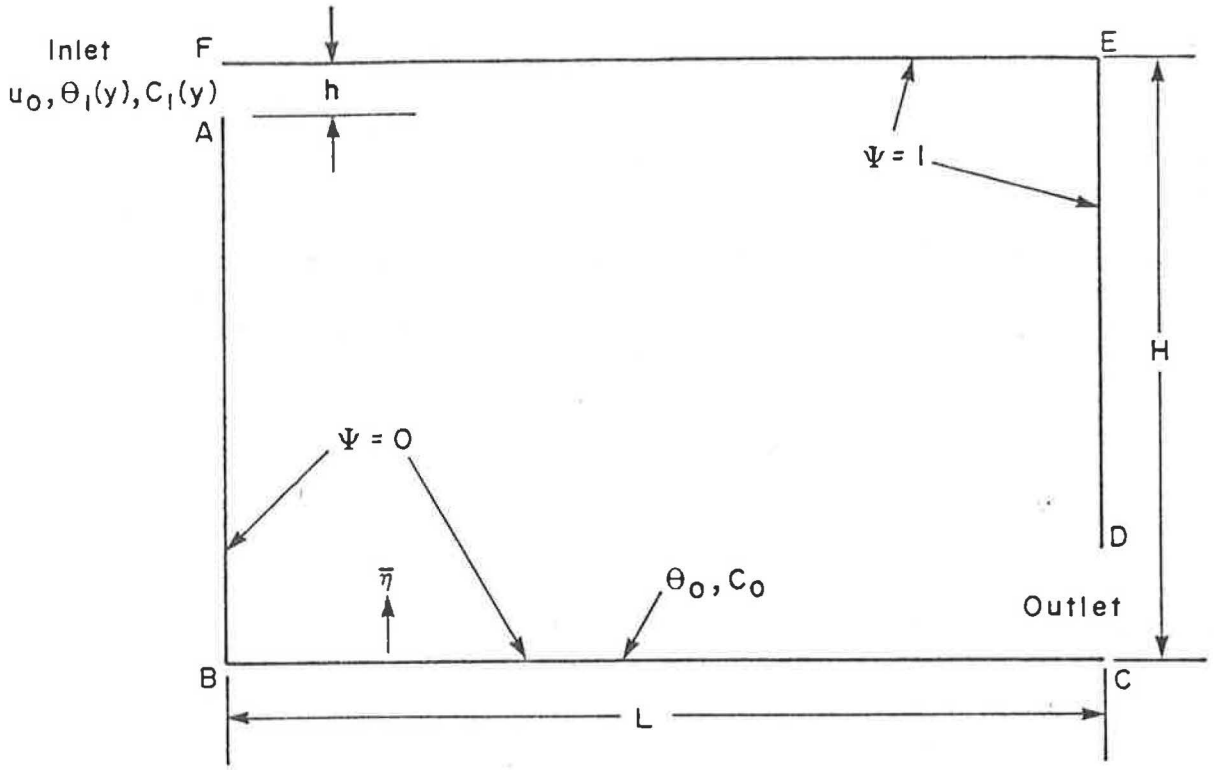

Fig. 2.1- Configuration of Room Model

3. THE GOVERNING EQUATIONS

We regard the contaminanted air in the two-dimensional ventilated airspace as a two-component system consisting of air and its low concentration gaseous or particle contaminant. When the heat and contaminant sources begin to diffuse, the flow is instantaneously disturbed. We assume a low concentration particle contaminant so that flow is perturbed only by momentum and buoyancy effects resulting from temperature gradients. Neglecting the heat generated by viscous dissipation and assume that the Boussinesq approximation applies; we seek solutions to the two-dimensional system of equations.

$$\frac{\partial C}{\partial t} + \frac{\partial uC}{\partial x} + \frac{\partial vC}{\partial y} = D \nabla^2 C \quad , \tag{3.1}$$

$$\frac{\partial \theta}{\partial t} + \frac{\partial u\theta}{\partial x} + \frac{\partial v\theta}{\partial y} = \alpha \nabla^2 \theta \quad , \tag{3.2}$$

$$\frac{\partial \omega}{\partial t} + \frac{\partial u\omega}{\partial x} + \frac{\partial v\omega}{\partial y} = \nu \nabla^2 \omega + \beta g \frac{\partial \bar{\theta}}{\partial x} \quad , \tag{3.3}$$

$$\nabla^2 \psi = -\omega \quad , \text{ and} \tag{3.4}$$

$$u = \frac{\partial \psi}{\partial x} \quad , \quad v = -\frac{\partial \psi}{\partial y} \tag{3.5}$$

where C is the contaminant concentration, θ the temperature, ω the vorticity, and ψ the streamfunction. u and v are the velocities in the horizontal x direction and the vertical y direction, respectively. β, D, α, ν are the constants of the flow field, representing the volume expansion coefficient, diffusivity, thermal diffusivity and kinematic viscosity, respectively.

By selecting the appropriate inlet parameters to characterize the flow in the ventilated airspace, Neilsen (1976) showed that the set of basic equations may be made dimensionless. In this study, the method is extended to include the concentration equation (3.1). Equation (3.1), (3.2), and (3.3) may be expressed in dimensionless form as

$$\frac{\partial C}{\partial t} + \frac{\partial uC}{\partial x} + \frac{\partial vC}{\partial y} = \frac{1}{Re\ Sc} \nabla^2 C \qquad (3.6)$$

$$\frac{\partial \theta}{\partial t} + \frac{\partial u\theta}{\partial x} + \frac{\partial v\theta}{\partial y} = \frac{1}{Re\ Pr} \nabla^2 \theta \qquad (3.7)$$

$$\frac{\partial \omega}{\partial t} + \frac{\partial u\omega}{\partial x} + \frac{\partial v\omega}{\partial y} = \frac{1}{Re} \nabla^2 \omega + \frac{Gr}{Re^2} \frac{\partial \bar{\theta}}{\partial x} \qquad (3.8)$$

Thus, according to the theory of similarity, the above dimensionless equations yield the following dimensionless terms:

$$Re = \frac{u_o h}{\nu_o} \qquad \text{Reynolds number} \qquad (3.9)$$

$$Sc = \frac{\nu_o}{D} \qquad \text{Schmidt number} \qquad (3.10)$$

$$Pr = \frac{\nu_o}{\alpha_o} \qquad \text{Prandtl number} \qquad (3.11)$$

$$Gr = \frac{\beta g \Delta \bar{\theta}_o h^3}{\nu_o^2} \qquad \text{Grashof number} \qquad (3.12)$$

The Archimedes number which is often used to characterize ventilation problems is expressed as

$$Ar = \frac{Gr}{Re^2} \qquad (3.13)$$

A numerical solution is sought for the finite difference form of equations 3.4 to 3.8 for the initial and boundary conditions considered below.

4. BOUNDARY CONDITIONS

The non-slip condition expressed as

$$u = \frac{\partial \psi}{\partial y} = o\ , \quad v = \frac{-\partial \psi}{\partial x} = o \qquad (4.1)$$

for the solid boundaries of the room geometry. If we specify the discharge flowrate to be unity, then we can arbitrarily set the two continuous wall streamfunctions to 0 and 1.0. Since the inlet velocity is uniform, the streamfunction across the inlet is then a linear function. The streamfunction at the outlet is not prescribed but obtained from known interior field by integrating the Poission equation (3.4).

The wall vorticity is approximated using Jensen's second order formula

$$\omega_w = \frac{(-7\,\psi_{i,w} + 8\,\psi_{i,w+1} - \psi_{i,w+2})}{2\,\Delta n^2} + O(\Delta n^2) \qquad (4.2)$$

Briley (1971) suggested that the use of equation (4.2) required the following formula to determine the velocity component u at points (i, w+1) adjacent to the wall

$$u_{i,w+1} = \frac{1}{4(\Delta n)}\,(-5\,\psi_{i,w} + 4\,\psi_{i,w+1} + \psi_{i,w+2}) \qquad (4.3)$$

The vorticity at the exit boundary is predicted from the interior using a cubic polynomial extrapolation of the form

$$\omega_m = -\omega_{m-4,j} + 4\,\omega_{m-3,j} - 6\omega_{m-2,j} + 4\omega_{m-1,j} \qquad (4.4)$$

The boundary conditions for normalized temperature on the wall is made simpler by assuming an adiabatic condition except at the floor where a value of 1 is arbitrarily specified. Roache (1971) showed that for the adiabatic wall, setting $\theta_{i,w} = \theta_{i,w+1}$ is computationally adiabatic and of second order accuracy. The inflow temperature profile is arbitrarily chosen as a linear function. The temperature at the outlet is treated in the same way as the vorticity.

The same remarks apply for the contaminant concentration boundary condition except at the non-source wall boundaries the concentration flux vanishes since we assume the contaminant cannot penetrate the surfaces and the sink mechanism is assumed to exist.

5. FINITE DIFFERENCE SCHEME

The governing equations (3.5 - 3.7) and (3.4 - 3.5) are solved by a finite difference scheme. The explicit preditor scheme has proved to be successful in studies of dynamic behaviour of incompressible flow in a two-dimension sudden expansion (Giaquinta 1974). The approach is here extended to study temperature and concentration field in addition to the flow field.

Equation (3.4), the Poission equation is solved by a successive over-relation iteration scheme; namely,

$$\psi_{i,j}^{k+1} = \psi_{i,j}^{k} + r\,(\tilde{\psi}_{i,j}^{k+1} - \psi_{i,j}^{k})$$

and

$$\tilde{\psi}^{k+1}_{i,j} = \frac{1}{R\left[1 + \left(\frac{\Delta x}{\Delta y}\right)^2\right]} \left\{ \psi^{k}_{i+1,j} + \psi^{k+1}_{i-1,j} + \left(\frac{\Delta x}{\Delta y}\right)^2 \left(\psi^{k}_{i,j+1} + \psi^{k+1}_{i,j-1} + (\Delta x)^2\, \omega_{i,j}\right)\right\}$$

where r is the relaxation coefficient, k is the number of iteration, i the horizontal grid index, j the vertical grid index, Δx is the horizontal grid size and Δy the vertical grid size.

The convergence criterion for equation (5.1) is

$$\frac{\text{Max} \mid \psi^{k+1}_{i,j} - \psi^{k}_{i,j} \mid}{\text{Max} \mid \psi^{k}_{i,j} \mid} < 0.0002$$

Equations (3.6 - 3.8) are formulated in the general form as

$$\xi^{n+1} = \xi^{n} + \Delta t \,.\, A \left(\frac{\partial^2 \xi^n}{\partial x^2} + \frac{\partial^2 \xi}{\partial y^2}\right) + \Delta t B \frac{\partial \xi^n}{\partial x} - \Delta t \left(\frac{\partial (u\xi)^n}{\partial x} + \frac{\partial (v\xi)^n}{\partial y}\right) + 0(\Delta t) \qquad (5.2)$$

where ξ is a general dependent variable representing C, θ and ω, and A and B is the appropriate dimensionless parameters, n represent the time level and $t^n = n \Delta t$. The central difference approximation of the convective terms in equation (5.2) is known to give rise to instabilities. Roache (1972) suggested the use of upwind differencing since the effect of perturbation is advected only in the direction of the velocity component at each point. Other researchers Gresho and Lee (1980) have observed that wiggles are unnecessarily suppressed by one-sided differencing. Combined upwind and central space approximation method are employed by introducing a parameter γ which determines the proportion of central space difference. An estimate of γ is obtained by

$$\gamma = \left(u \frac{\Delta t}{\Delta x} + v \frac{\Delta t}{\Delta y}\right) \max \qquad (5.3)$$

A second upwind differencing method based on the Donor Cell approach is used by computing interface velocities. This technique retains something of the second order accuracy for central space differencing.

A further improvement to the explicit scheme is obtained by including a corrector step to the algorithm such that the scheme is then second order in time. Ames (1973) applied this method to a one-dimensional non-linear diffusion equation.

The significant change in the vorticity field is accounted by setting a convergence criteria of the form

$$\left| \frac{\sum_{i,j} | \omega_{i,j} |}{\frac{1}{\Delta x^2} \sum_{i,j} | \psi_{i+1,j} + \psi_{i-1,j} + \gamma_o^2 (\psi_{i,j+1} + \psi_{i,j-1}) - 2(1 - \gamma_o^2) \psi_{i,j} |} \right| \leq \epsilon_1$$

where $\gamma_o = (\frac{\Delta x}{\Delta y})$ and ϵ_1 is determined by computation experimentation. Premature convergence is detected by imposing the following criteria:

$$\frac{|\omega_{i,j}^{n+1} - \omega_{i,j}^{n}|_{max}}{|\omega_{i,j}^{n}|_{max}} \leq \epsilon_2$$

Numerical convergence is established by examining plots of ϵ_1 and ϵ_2 with time.

6. RESULTS

The computational algorithm was tested numerically against Giaquinta (1974) studies on laminar flow of an incompressible fluid through a two-dimensional sudden expansion. Similar steady state flow fields for Reynolds numbers of 10 and 100 were obtained when convergence was obtained after satisfying Poiseuille flow conditions at the downstream exit boundary. The algorithm was then extended to a ventilated airspace for a room geometry as shown in Figure 2.1.

The magnitude of the time increment used initially was calculated from the diffusion characteristics of the flow by the dynamic stability criterion obtained using the quasilinear analysis of Lax and Richtmyer (1956). A number of numerical runs led to the conclusion that the time increment had to be an order of magnitude less than given by the stability criteria. Smooth variation of the vorticity resulted when the time step, $\Delta t = 0.000125$, was used. This time step was periodically increased as the solution progressed. The numerical experiments for varying conditions were restricted for two cases with data given in the table below.

Data	Value
Reynolds number (Re)	100., 1000.
Grashof number (Gr)	1000.
Schmidt number (Sc)	1.
Prandtl number (Pr)	1.0
U_o at inlet	2.0
Heat and concentration line source at the floor	1.0
Heat and concentration point source at inlet	0.5

The potential solution ($\nabla^2\psi = 0$) was initally used as an approximation of the streamfunction solution at the impulsive start. At the impulsive start vorticity was introduced into the flow and at the sametime the concentration and temperature sources simultaneously begin to operate. Although the transient development of flow and mass and heat transfer characteristics of the separated flow impulsively started from rest are available, it is the numerical converged solution that is of interest in this study. Numerical convergence ($\epsilon < 0.0002$) was obtained after a large number of iterations with the small time step required in the explicit scheme. Even with numerical convergence, there is some doubt whether steady state flow conditions prevails expecially with respect to heat and mass convection and diffusion.

A searching routine was used to search for all points at which a vertical or horizontal grid line intersects the prescribed value of the variable (e.g., streamline) desired. Several representative contours were drawn to characterize the separated flow, heat, and concentration function in the ventilated airspace.

Case 1. Re = 100, Gr = 1000, Pr = 1, Sc = 1.

Initally, a series of computations were run to study the behaviour of the contaminant concentration and temperature profile in the ventilated airspace for Archimedes number ($Ar = Gr/Re^2$) Ar = 0.1. This is in the range of parameters in flows of practical living quarters with Rayleigh number ($Ra = Gr.Pr$) in excess of $Ra \leq 10^4$.

The streamline patterns indicate a pronounced eddy zone at the lower left hand cornor as shown in figure (6.1). The bounding streamline of the eddy is shown separating from the edge of the inlet orifice.

Resultant velocities line of equal magnitude are shown in figure (6.2). The back flow phenomenon is illustrated within the eddy zone. The vertical wall boundary has the tendency of suppressing the longitudinal velocity component in the eddy zone. Deaccelerating and accelerating effect on the magnitude of the velocity profile are noted for the inlet and outlet port, respectively.

The iso-vorticity contours are represented in figure (6.3). The uncertainty in the vorticity contours at the inlet and outlet region are characterized by void spaces. Separation and rejoining of iso-vorticity lines are noted on both horizontal and vertical wall boundaries.

The temperature and concentration profiles are shown in figure (6.4) and (6.5). They are inherently similar as described by the governing equations. Buoyancy effects are noted in the eddy zone and the region where momentum effects are minimal. Low temperature and concentration distribution occur at the upper right hand corner region because of its proximity in the high flow field.

Case II. Re = 1000, Gr = 1000, Pr = 1.0, Sc = 1.0

The ventilated air space is investigated for Archimedes number Ar = 0.001 or Rayleigh number $Ra = 10^6$. The primary and secondary eddy zones occupied most of the flow field as can be seen in Figure (6.6). The streamlines above the eddy zones appear to follow the top wall boundary before converging towards

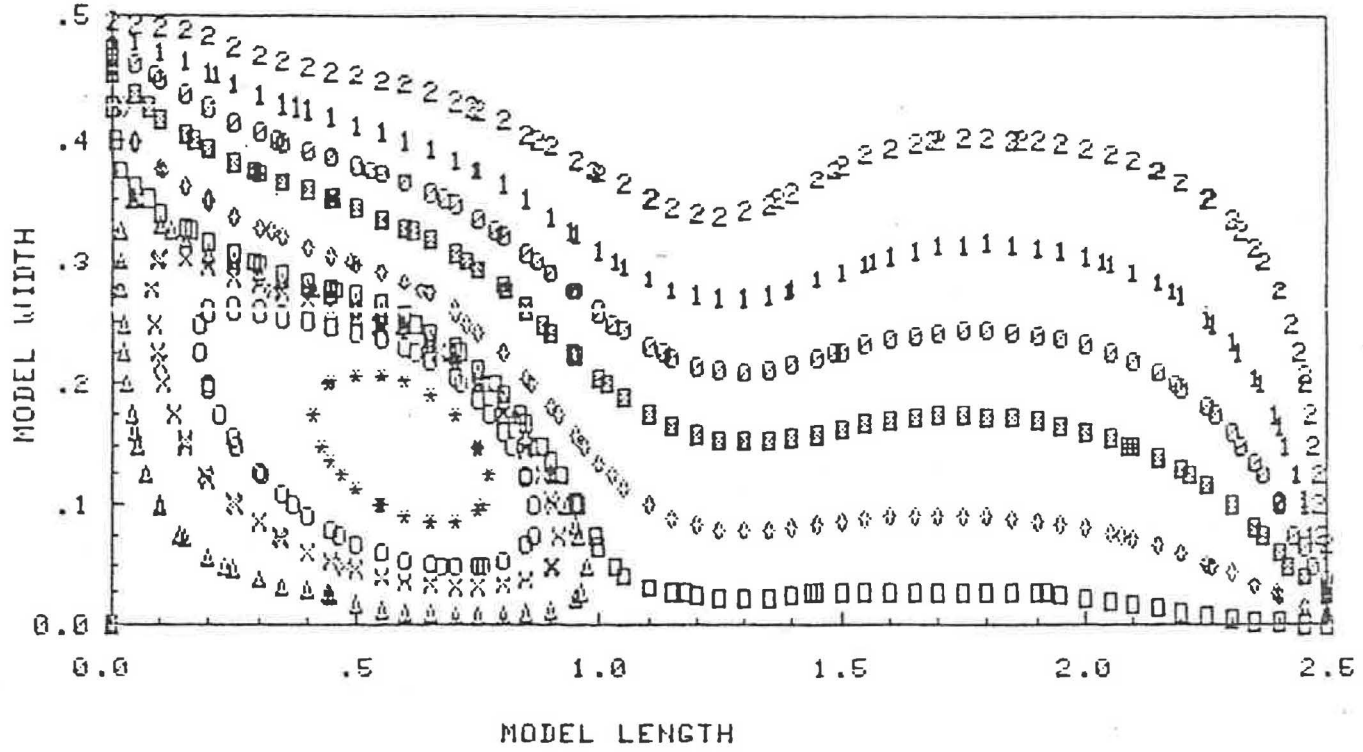

LEGEND

Symbol	ψ
*	-0.01
O	-0.05
X	-0.025
Δ	-0.005
□	0.01
◊	0.1
■	0.3
Ø	0.5
1	0.7
2	0.9

Figure 6.1 Streamlines Flow Patterns at Numerical Convergence
Re=100 Gr=1000 Pr= 1.0 Sc=1.0

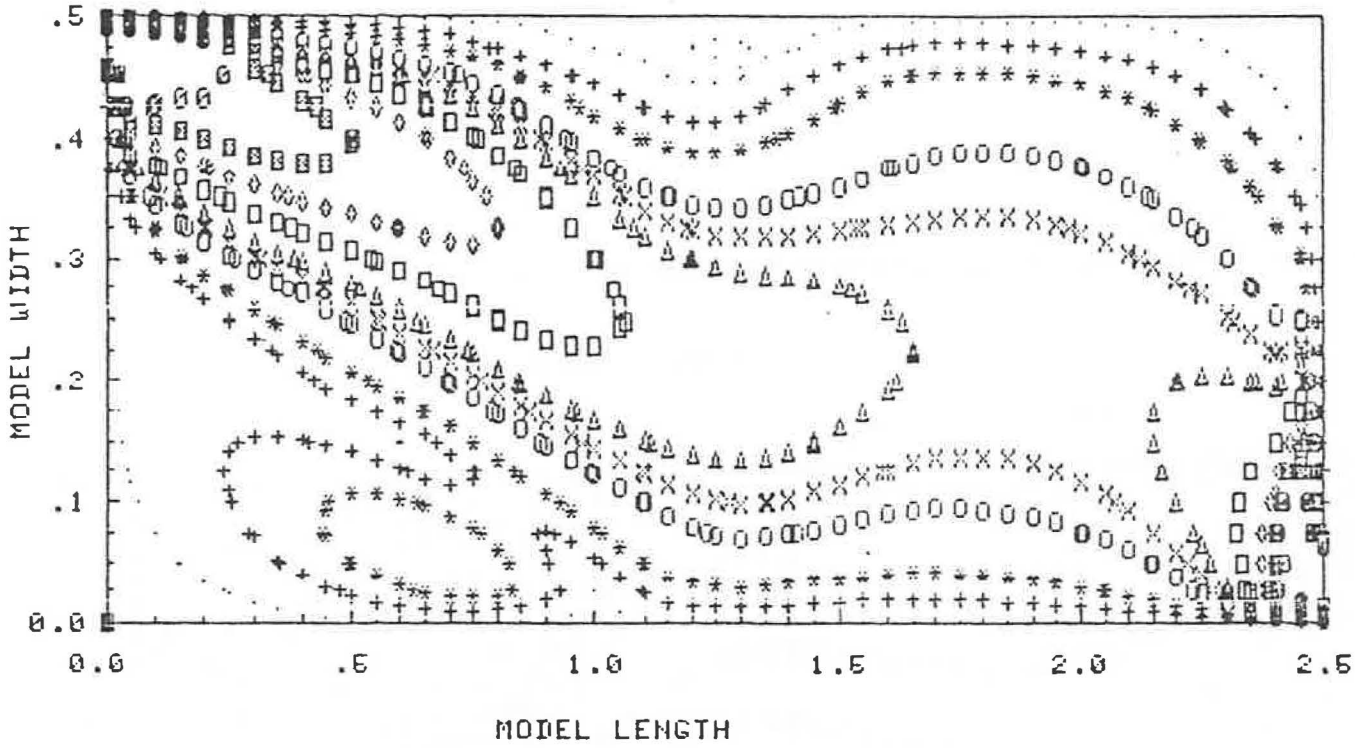

LEGEND

Symbol	$\bar{v}$
·	0.1
+	0.5
*	1.0
O	2.0
X	2.5
Δ	3.0
□	4.0
◊	5.0
⊠	6.0
Ø	7.0

Figure 6.2 Resultant Velocity Profiles at Numerical Convergence
Re=100 Gr=1000 Pr=1.0 Sc=1.0

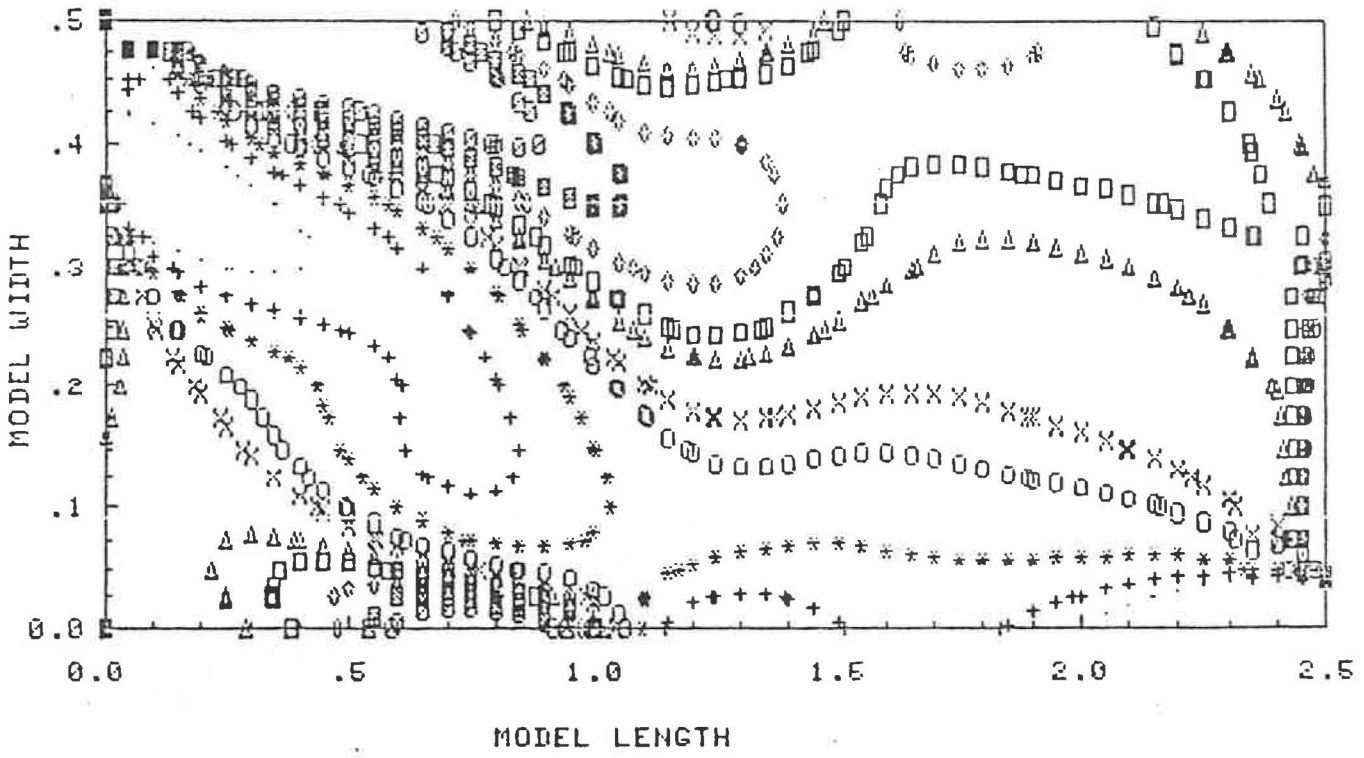

Figure 6.3 Vorticity Contours at Numerical Convergence
Re=100 Gr=1000 Pr=1.0 Sc=1.0

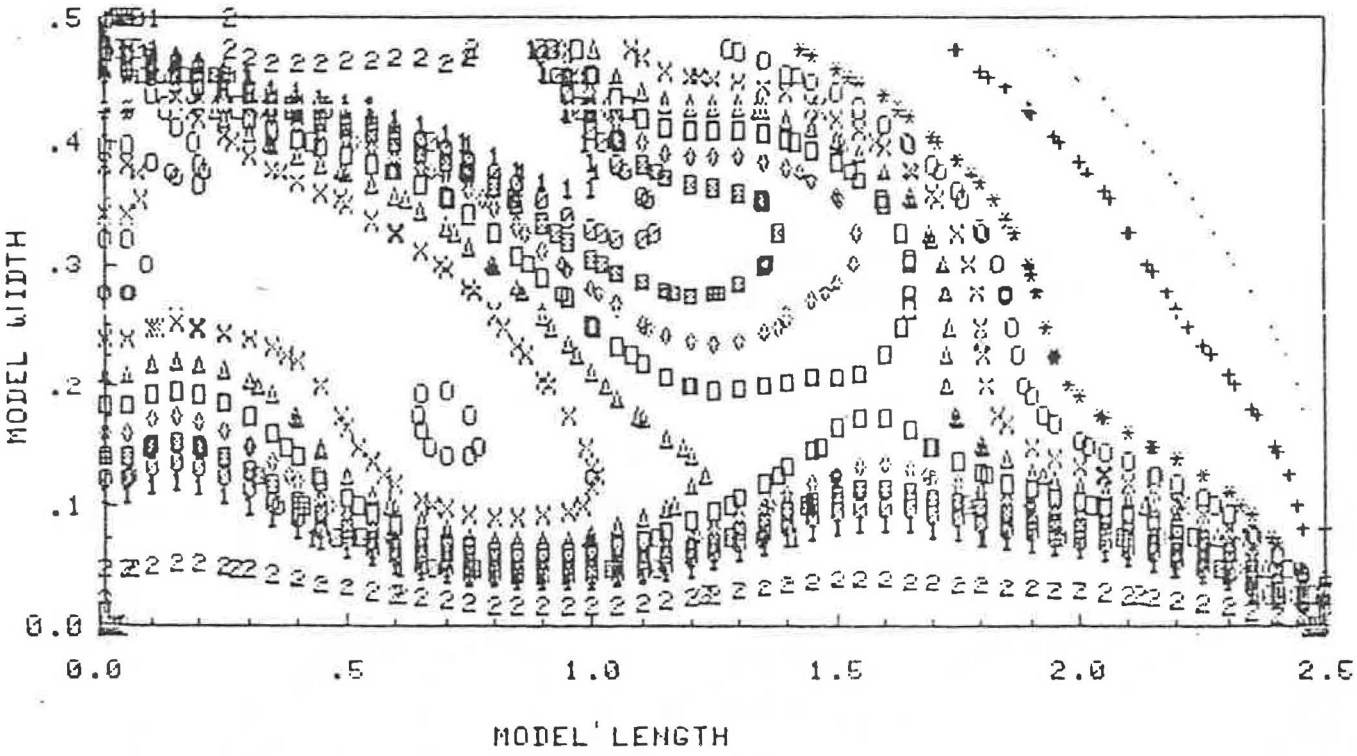

LEGEND

Symbol	θ
·	0.001
+	0.01
*	0.1
O	0.15
X	0.2
Δ	0.25
□	0.3
◊	0.35
▣	0.4
Ø	0.45
1	0.5
2	0.7

Figure 6.4 Temperature Profiles at Numerical Convergence
Re=100 Gr=1000 Pr=1.0 Sc=1.0

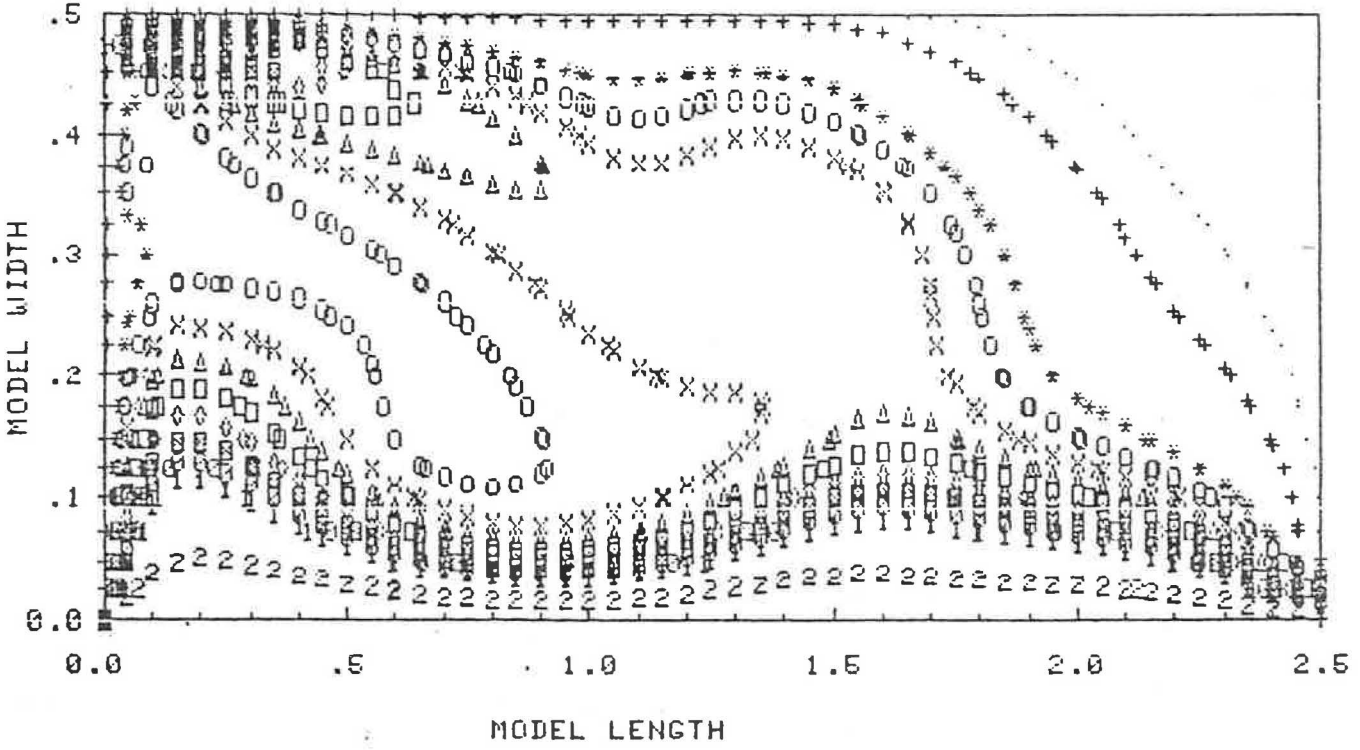

LEGEND

Symbol	C
·	0.001
+	0.01
*	0.1
O	0.15
X	0.2
Δ	0.25
□	0.3
◈	0.35
▣	0.4
Ø	0.45
1	0.5
2	0.7

Figure 6.5 Concentration Profiles at Numerical Convergence
Re=100 Gr=1000 Pr=1.0 Sc=1.0

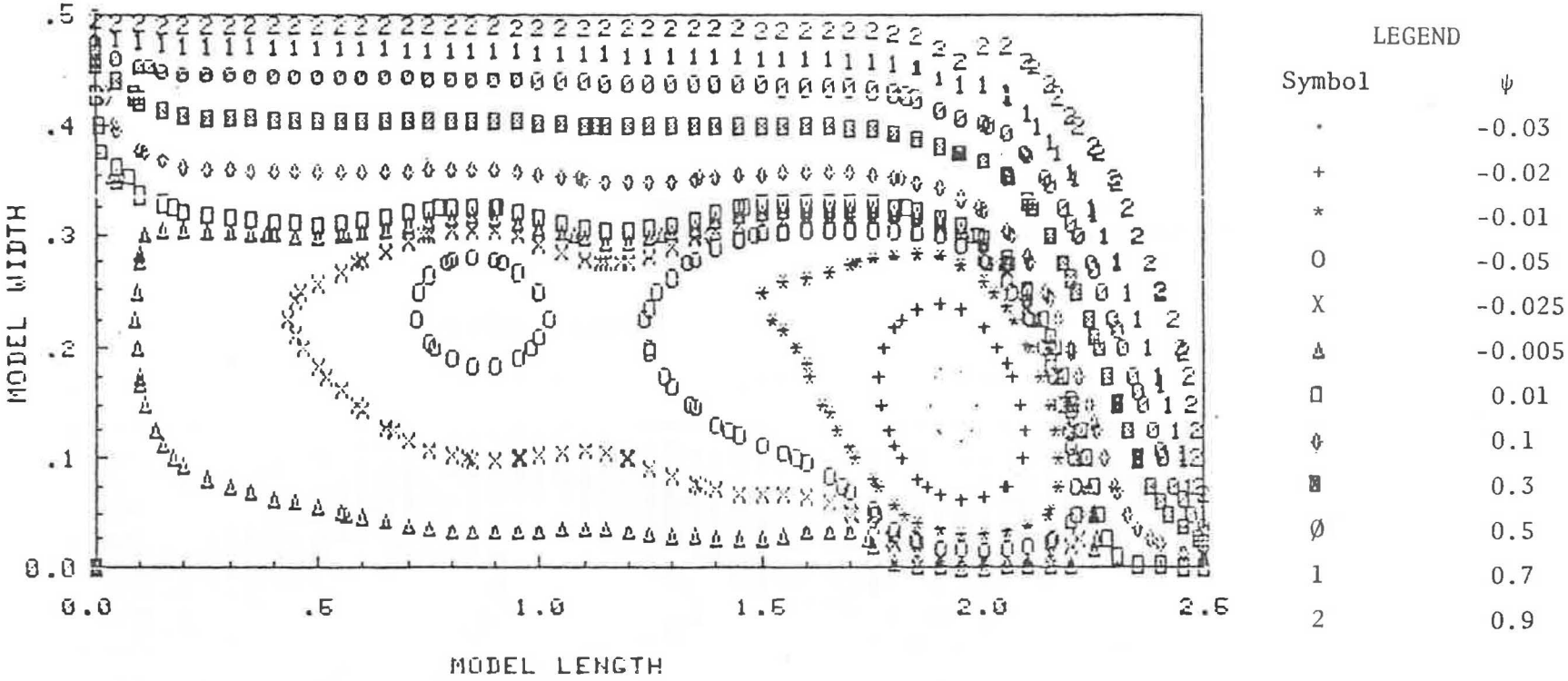

Figure 6.6 Streamfunction Flow Patterns at Numerical Convergence
Re=1000 Gr=1000 Pr=1.0 Sc=1.0

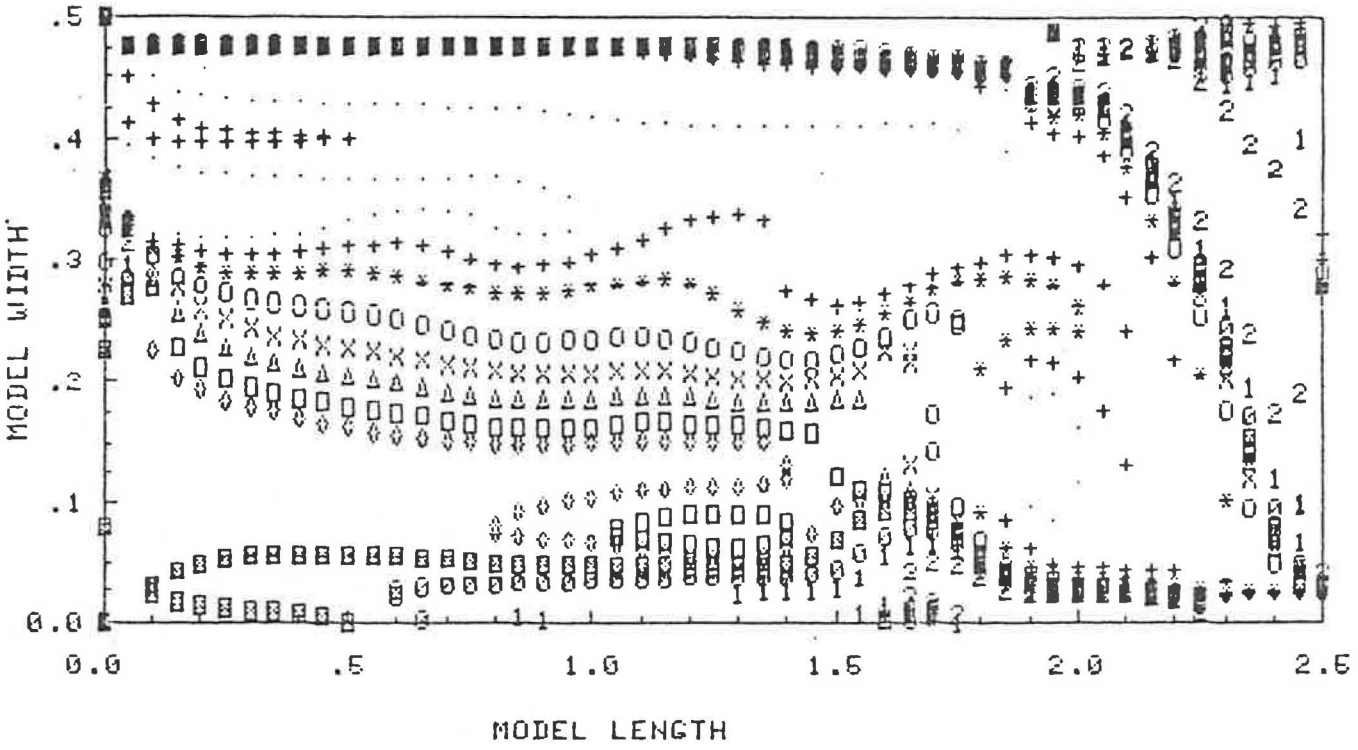

LEGEND

Symbol	θ
·	-30.
+	-20.
*	-10.
O	-1.0
X	-0.001
Δ	0.01
□	0.1
◊	1.0
■	10.
1	20.
2	30.

Figure 6.8 Vorticity Profile at Numerical Convergence
Re=1000 Gr=1000 Pr=1.0 Sc=1.0

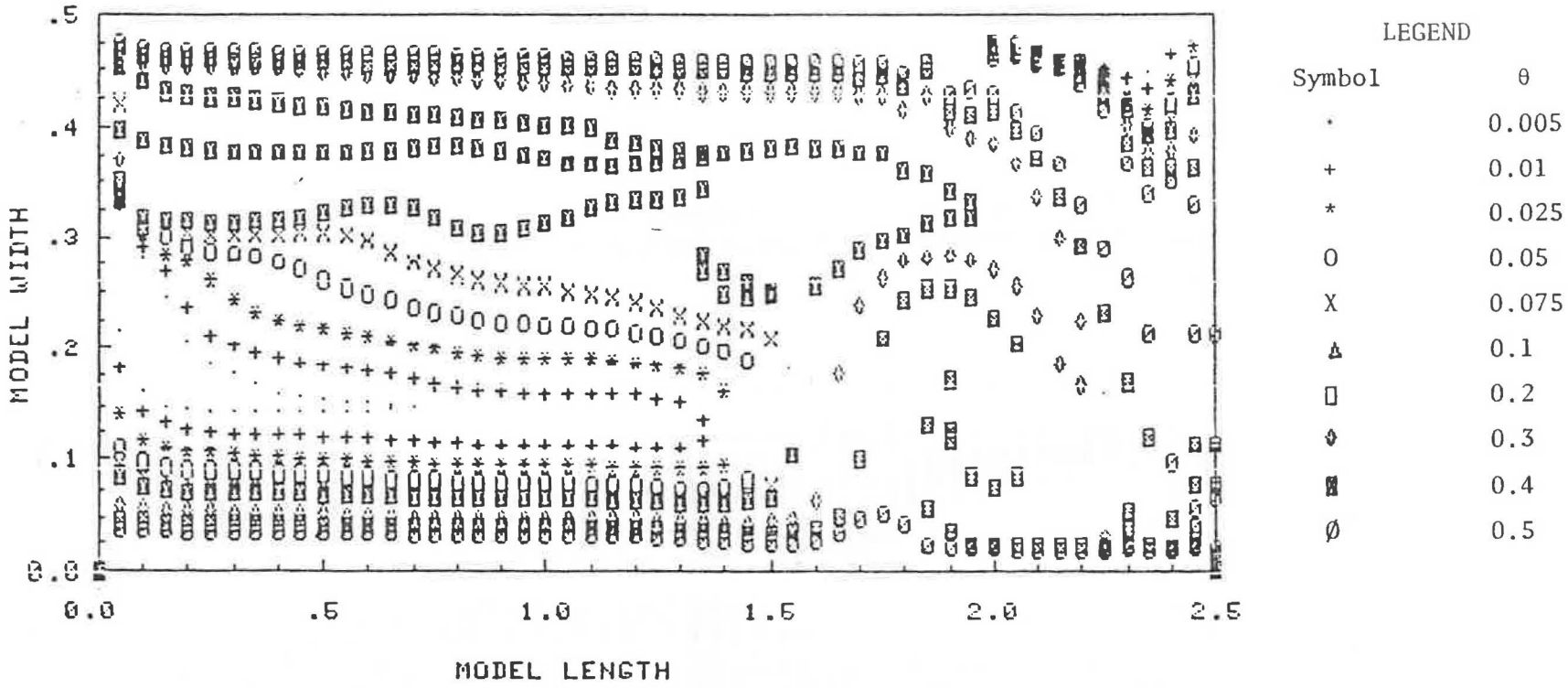

Figure 6.9 Temperature Profiles at Numerical Convergence
Re=1000 Gr=1000 Pr=1.0 Sc-1.0

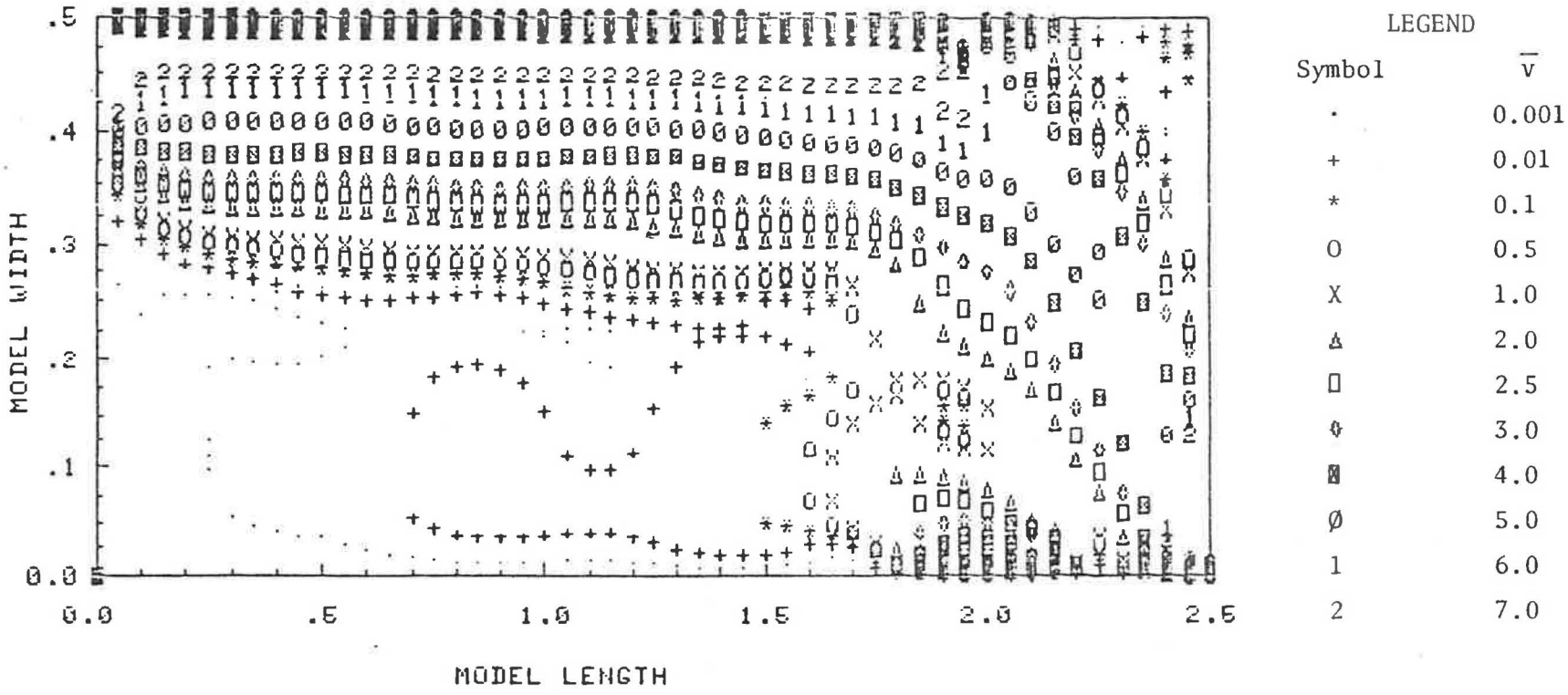

Figure 6.7 Resultant Velocity Profiles at Numerical Convergence
Re=1000 Gr=1000 Pr=1.0 Sc=1.0

the outlet. Similar characteristics are observed in the velocity profiles of equal magnitude. Irregularities and scatter of low velocity values occurred in the eddy zones.

Separation of iso-vorticity lines predominates for these range of parameters and only search of iso-vorticity values along the longitudinal direction of motion can be presented, see Figure (6.8). Although there is much scatter some continuity is observed in the central region of the eddy zones. Some recirculation of iso-vorticity lines are noted at the primary eddy zone.

The temperature and concentration profiles using longitudinal search routine are shown in Figure (6.9) and (6.10) respectively. Interaction of the point inlet source and the floor line source is seen in a zone of turbulent mixing at the primary eddy (see Figure 6.6). Buoyancy effects are minimal because of the high flow rate or Reynolds number. The top right hand corner have high temperatures and concentration values for these conditions.

The heat rate for Case I and II for the line source on the floor is represented in Figure 6.11 and 6.12 respectively. In the first case (Re = 100) buoyancy effects are more pronounced while momentum is less important and hence low Nusselt number are noted. The zone of high Nussult number corresponds to the location where the jet from the inlet reaches the floor. The valley in Figure (6.12), however, corresponds to the stagnation interaction of the longitudinal jet from the inlet and the accelerating effects of the outlet.

7. Discussion

From the results, we noted the behavior of temperature and low concentration contaminant in the operating range of parameters of a ventilated air space. Steady flow assumptions at numerical convergence may be valid for the given room geometry with no heat or concentration source. There is some doubt, however, whether the steady-state condition exists for a mixed type of ventilated problem as numerical convergence for heat and mass transfer need not be identical to that which was used for fluid flow.

Two dimensional flow studies and the necessary assumptions of constant dimensionless parameters are useful for qualitative study of the ventilated problem and provide better understanding of the actual physical phenomena, however much more work is necessary to provide quantitative comparisons with experimental data.

Nonetheless the present results help explain the physical behavior of complex fluid flow phenomena in two dimensional spaces with heat and mass transfer interactions.

Acknowledgement

The authors are grateful to Professor G.E. Zoerb for financial assistance.

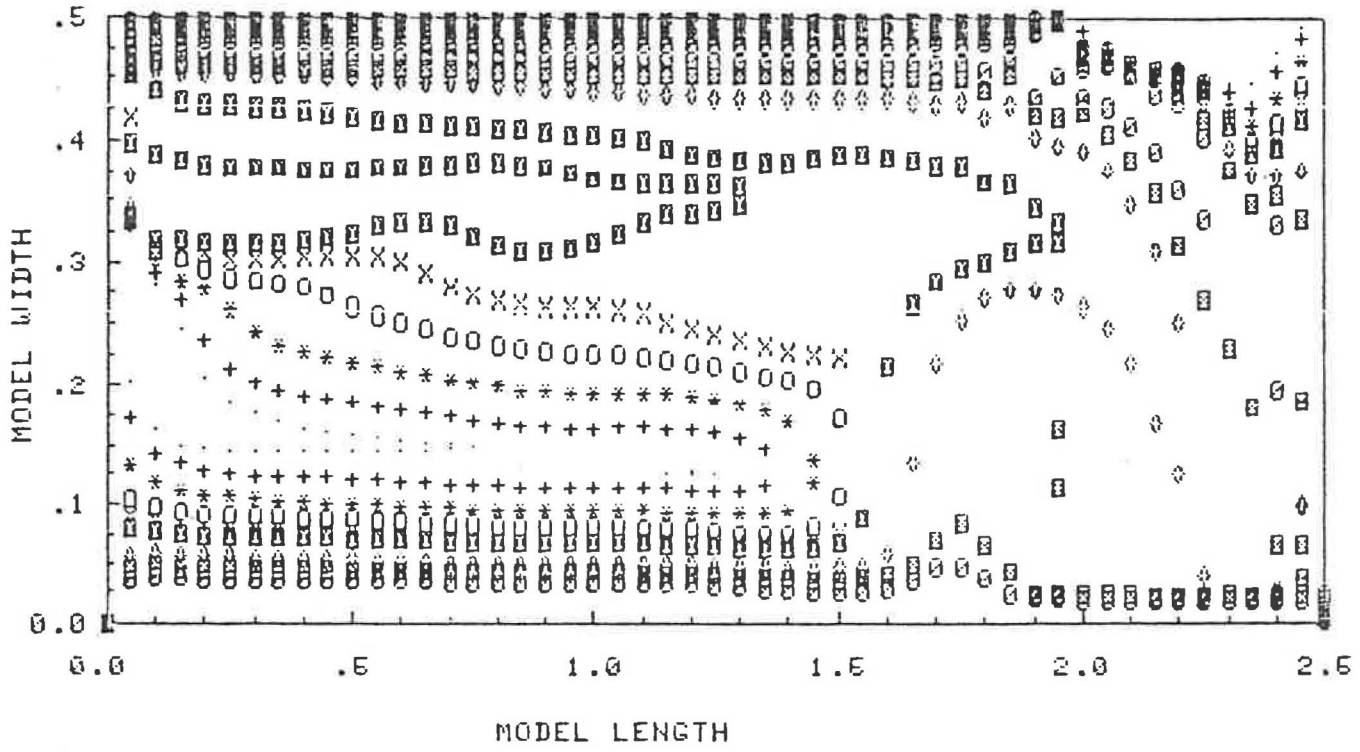

LEGEND

Symbol	C
·	0.005
+	0.01
*	0.025
O	0.05
X	0.075
△	0.1
□	0.2
◊	0.3
■	0.4
Ø	0.5

Figure 6.10 Concentration Profiles at Numerical Convergence
Re=1000 Gr=1000 Pr=1.00 Sc=1.0

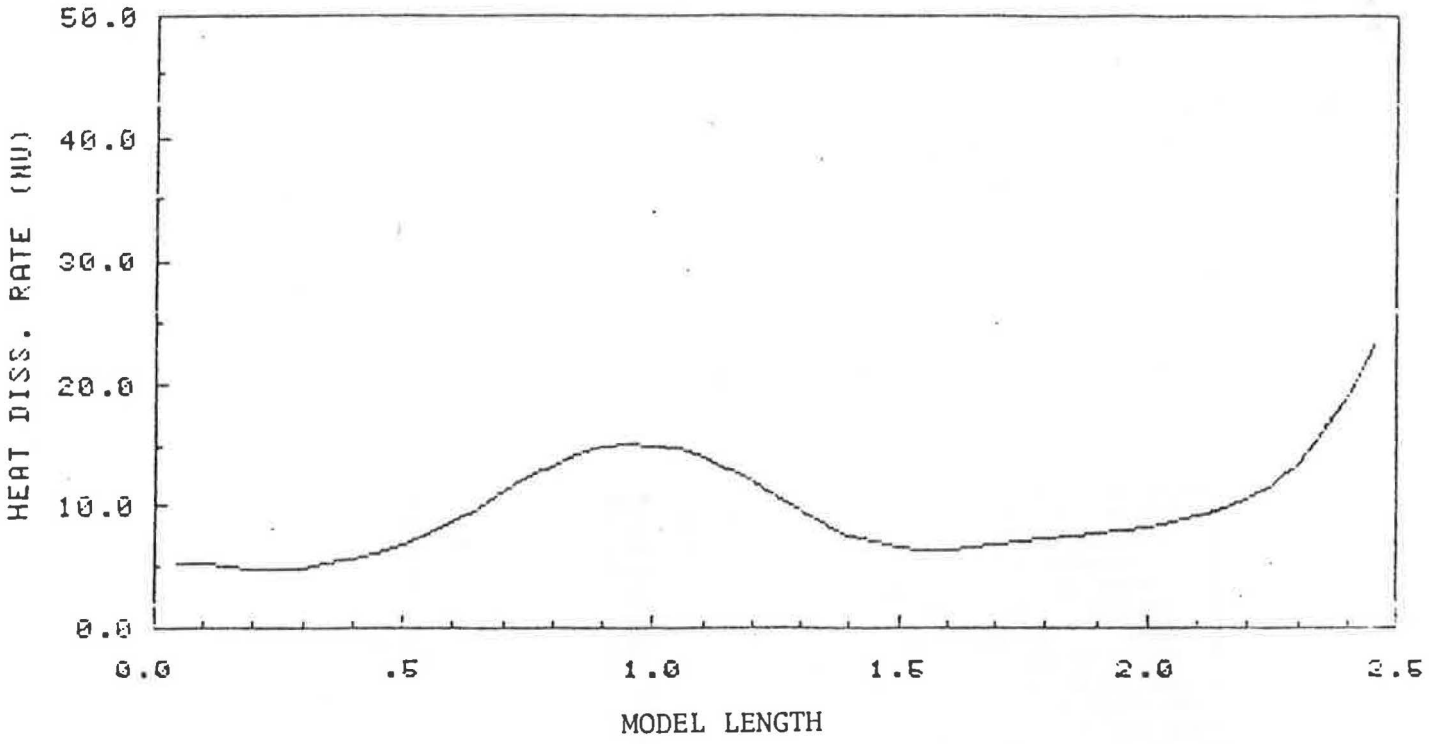

Figure 6.11 Heat rate of floor surfaces in terms of Nussult Number (Nu)

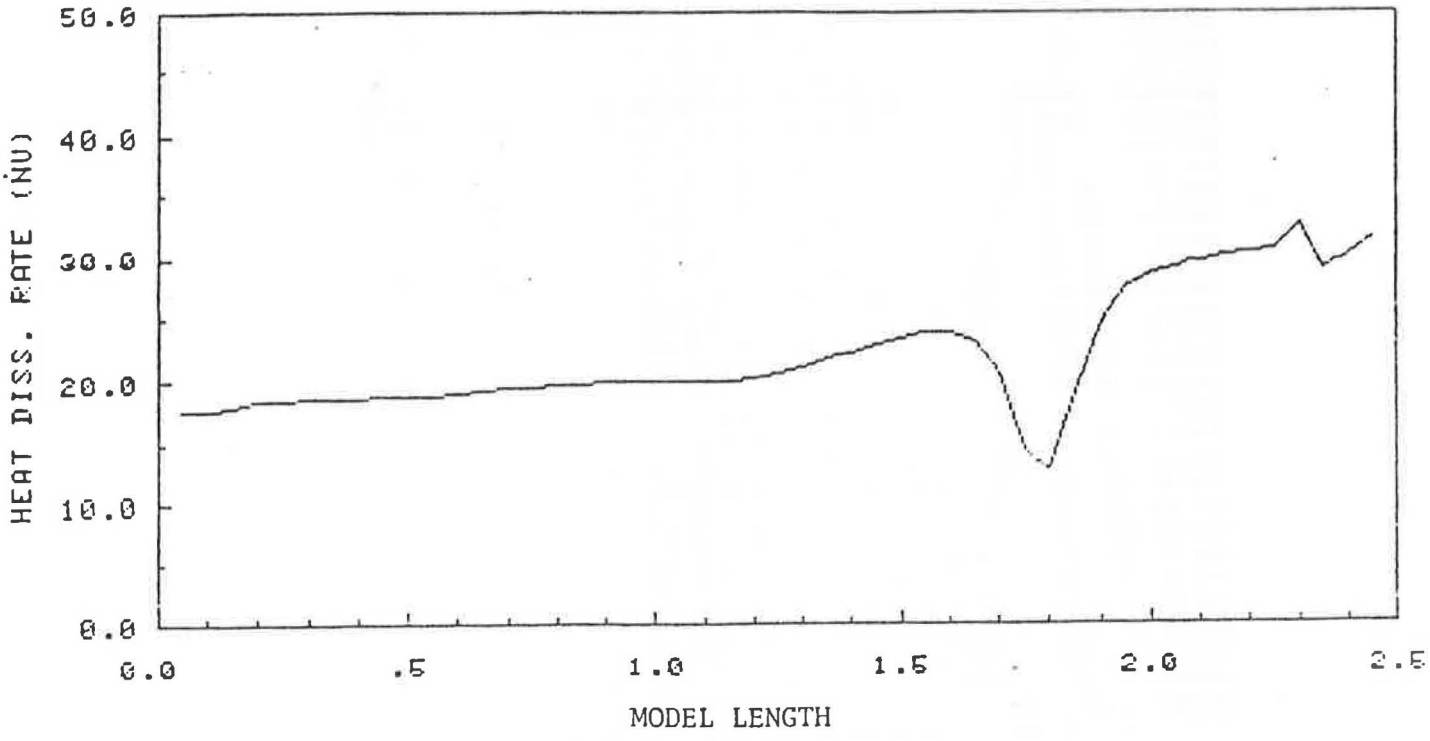

Figure 6.12 Heat rate at floor surface in terms of Nussult number (Nu)

References

1. Ames, W.F. (1973). Computational Steeples in Fluid Mechanics, SIAM Review, Vol. 15, No. 2, pp. 524 - 552.

2. Briley, R.W. (1970). A Numerical Study of Laminar Separation Bubbles Using Navier-Stokes Equations. J. Fluid Mech. Vol. 47, Part 4, pp. 713 - 736.

3. Giaquinta, A.R. (1974). Numerical Modelling of Unsteady Flow with Natural and Forced Separation, Ph.D. Dissertation, Univ. of Iowa, Iowa.

4. Gresho, P.M. and R.L. Lee (1980). Don't Suppress the Wiggles - They are Telling you Something. UCRL - 82979. Lawrence Livermore Laboratory, Univ. of California, Livermore.

5. Launder, B.E., D.B. Spalding and J.H. Whitelaw, (1973). Turbulence Models and Their Experiment Verifications, Imperial College, Mech. Eng.

6. Lax, P.D. and Richtmyer, R.D. (1956). Survey of the Stability of Linear Finite Difference Equations, Comm. Pure Appl. Math, Vol. 9, pp. 267-293.

7. Lumley, J.L. and Panosky, H.A. (1964). The Structure of Atmospheric Turbulence. Interscience Publishers, N.Y.

8. Nielsen, P.V., A. Restivo and J.H. Whitelaw (1979). Buoyancy-affected Flows in Ventilated Rooms. Numerical Heat Transfer, Vol. 2, pp. 115 - 127.

9. Nielsen, P.V. (1976). Flow in Air Conditioned Rooms. Ph.D. Dissertation, Technical Univ. of Denmark, Denmark.

10. Roache, P.J. (1972). Computational Fluid Dynamics, Hermosa Publishers, Albuquerque, New Mexico.

11. Timmons, M.B. (1979). Experimental and Numerical Study of Air Movement in Slot-Ventilated Enclosures. Ph.D. Dissertation, Cornell Univ. N.Y.